FasR regulates fatty acid biosynthesis and is essential for virulence of *Mycobacterium tuberculosis*

Sonia Mondino[1&,#a], Cristina Lourdes Vázquez[2&], Matías Cabruja[1&,#b], Claudia Sala[3,#c], Amaury Cazenave-Gassiot[4], Federico Carlos Blanco[2], Markus R. Wenk[4], Fabiana Bigi[2], Stewart T. Cole[3,#a], Hugo Gramajo[1] and Gabriela Gago[1*]

1- Laboratory of Physiology and Genetics of Actinomycetes, Instituto de Biología Molecular y Celular de Rosario (IBR-CONICET), Facultad de Ciencias Bioquímicas y Farmacéuticas, Universidad Nacional de Rosario, Rosario (2000), Argentina

2- Instituto de Biotecnología-IABIMO, UEDD CONICET-Instituto Nacional de Tecnología Agropecuaria (INTA), Argentina.

3- Global Health Institute, Ecole Polytechnique Fédérale de Lausanne, Lausanne, Switzerland.

4- Singapore Lipidomics Incubator (SLING), Life Sciences Institute, and Department of Biochemistry, Yong Loo Lin School of Medicine, National University of Singapore, Singapore.

[#a] Current address: Institut Pasteur, Paris (France)

[#b] Current address: Stanford University (United States)

[#c] Current address: Fondazione Toscana Life Sciences, Siena (Italy)

* Corresponding author

E-mail: gago@ibr-conicet.gov.ar (GG)

[&] These authors contributed equally to this work

Abstract

Mycobacterium tuberculosis, the etiologic agent of human tuberculosis, is the world's leading cause of death from an infectious disease. One of the main features of this pathogen is the complex and dynamic lipid composition of the cell envelope, which adapts to the variable host environment and defines the fate of infection by actively interacting with and modulating immune responses. Fine regulation of *de novo* fatty acid biosynthesis, and its interaction with other peripheral lipid pathways, is essential for cell membrane homeostasis while quickly adapting to the growth environment. However, while much has been learned about the enzymes of the numerous lipid pathways present in *M. tuberculosis,* little knowledge is available regarding the proteins and metabolic signals regulating lipid metabolism during infection. Previous studies on the regulation of lipid biosynthesis in mycobacteria identified FasR as an essential transcriptional activator of *de novo* fatty acid biosynthesis in *Mycobacterium smegmatis*. In this work, we constructed and characterized a FasR-deficient mutant in *M. tuberculosis* and demonstrated that FasR positively regulates *fas* and *acpS* expression. Lipidomic analysis of the wild type and mutant strains revealed complete rearrangement of most lipid components of the cell envelope, with phospholipids, mycolic acids, sulfolipids and phthiocerol dimycocerosates relative abundance severely altered. As a consequence, replication of the mutant strain was impaired in macrophages leading to reduced virulence in a mouse model of infection. Moreover, we show that the *fasR* mutant resides in acidified cellular compartments, suggesting that the

lipid perturbation caused by the mutation prevented *M. tuberculosis* inhibition of phagolysosome maturation. This study identified FasR as a novel factor involved in regulation of mycobacterial virulence and provides evidence for the essential role that modulation of lipid homeostasis plays in the outcome of *M. tuberculosis* infection.

Author summary

Tuberculosis is the leading cause of death from a single infectious disease, resulting in approximately 1.5 million deaths per year worldwide. The composition and complexity of the cell envelope is the most distinctive feature of *Mycobacterium tuberculosis*, the etiologic agent of human tuberculosis. As the mycobacterial cell envelope is the interface with the host, the modulation of its structure and consequent responsiveness to immune factors might be important in determining the state of an infection. We have previously identified FasR as an essential transcriptional activator of *de novo* fatty acid biosynthesis in *Mycobacterium smegmatis*. In this study, a *M. tuberculosis* mutant strain in *fasR* was constructed and analyzed. Inactivation of *fasR* in *M. tuberculosis* was not lethal for *in vitro* growth but led to rearrangement of the lipid composition of the cell envelope. Consequently, the mutant strain was less virulent in a mouse model of infection and showed impaired replication in macrophages, thus implying that lipid homeostasis plays an important role during *M. tuberculosis* infection.

Introduction

Tuberculosis (TB) is one of the top ten causes of death and the leading cause from a single infectious agent, exceeding both malaria and HIV. In 2018, there were an estimated 10 million new cases of active TB and 1.3 million patients died from active infection [1]. The emergence of multidrug-resistant TB (MDR-TB) presents an increasingly difficult therapeutic challenge; consequently, MDR-TB is now the main cause of death due to antimicrobial resistance [1] thus transforming this long neglected disease into a global health priority.

The composition and complexity of the cell envelope is the most distinctive feature of *Mycobacterium tuberculosis*, the etiologic agent of human TB. Biochemical and microscopic data revealed that the mycobacterial envelope consists of three discrete entities: a plasma membrane surrounded by a complex cell wall and an outermost layer called the capsule in pathogenic species [2,3]. The *M. tuberculosis* cell wall consists of peptidoglycan covalently linked to arabinogalactan esterified by mycolic acids (MA), which form the inner leaflet of the outer membrane bilayer (mycomembrane). The outer leaflet of this membrane is composed of free, non-covalently bound lipids and glycolipids like trehalose monomycolates (TMM), trehalose dimycolates (TDM), glycerol monomycolates, glucose monomycolates, phthiocerol dimycocerosates (PDIM), poly acylated trehaloses (PAT), sulfolipids (SL), phosphatidylinositol mannosides (PIM), phenolic glycolipids (PGL) and mannose-capped lipoarabinomannans (Man-Lam) [4,5].

During the course of infection, intracellular pathogenic bacteria use different strategies to survive, multiply and persist inside the host [6]. *M. tuberculosis*

98 encounters heterogeneous host environments, including high oxygen tension in the
99 lung alveolus, reactive oxygen and nitrogen species in activated macrophages, as
100 well as nutrient depletion and hypoxia in tuberculous granulomas. How *M.*
101 *tuberculosis* survives these diverse environments is not fully understood. *M.*
102 *tuberculosis* has evolved a wide array of specific lipids and related metabolic
103 pathways that actively interact with the immune system, and multiple reports from
104 human and animal studies suggest an intimate link between *M. tuberculosis* lipid
105 metabolism and outcome of infection [7–9]. Of particular interest is the challenge
106 that *M. tuberculosis* must face in order to adjust its own lipid metabolism while the
107 macrophage is changing its lipid content [10]. Little is known about the mechanism
108 underlying the reorganization of *M. tuberculosis* envelope during infection [11].
109 Understanding how this pathogen selects and organizes the envelope components
110 to resist killing, and how these components make the envelope essential to *M.*
111 *tuberculosis* survival, virulence and pathogenesis, is still a major challenge.
112 Therefore, characterization of the regulatory elements that control these processes
113 should help improve understanding of the mechanisms involved in mycobacterial
114 pathogenicity and could provide new potential targets for anti-TB chemotherapy.
115 Previous studies on the regulation of lipid biosynthesis in mycobacteria allowed us
116 to identify FasR as the transcriptional activator of fatty acid biosynthesis in *M.*
117 *smegmatis* [12]. Deletion of *fasR* from *M. smegmatis* was possible only in the
118 presence of an extra copy of the gene, suggesting that *fasR* is essential for
119 viability. Notably, we found that the affinity of FasR for its target promoter is
120 modulated by long chain acyl-CoAs ($\geq C_{16}$), the end products of the FAS I pathway.
121 FasR, together with MabR, the transcriptional regulator of MA biosynthesis, are the

122 only transcription factors involved in fatty acid biosynthesis regulation known to be
123 essential for *M. smegmatis* survival, reflecting the relevance of lipid homeostasis
124 for mycobacterial viability [12,13].
125 In this study, a *M. tuberculosis* knockout strain in *fasR* was constructed and the
126 mutant used to analyze the implications of lipid homeostasis in *M. tuberculosis*
127 virulence. Inactivation of *fasR* in *M*. *tuberculosis* was not lethal for *in vitro* growth
128 but led to complete rearrangement of lipid composition of the envelope.
129 Consequently, the mutant strain was less virulent in a mouse model and showed
130 impaired replication in macrophages, thus implying that lipid homeostasis plays an
131 important role during *M. tuberculosis* infection.
132

133 ## Results

134

135 **Construction and characterization of *M. tuberculosis fasR* mutant strain**

136 To investigate the function of FasR in *M. tuberculosis,* and considering that *fasR* is
137 essential for *M. smegmatis* viability, we first constructed an *M. tuberculosis*
138 conditional knockdown strain in *fasR* (Fig 1A-B). Plasmids pFR33, providing a
139 second copy of *fasR* under the control of the TET-PIP OFF system at the
140 chromosomal L5 phage attachment site *attB* [14] and pGA80, were simultaneously
141 transformed in *M. tuberculosis* (S1 Table). Disruption of *fasR* was then obtained by
142 two-step allelic exchange using pFR35, which deleted the gene at the native locus.
143 Homologous recombination was confirmed by colony PCR and Southern blot
144 analysis, and the resulting conditional knockdown strain was named *Mtb*Δ*fasR*-

145 c*fasR* (Fig 1D). In this strain, expression of *fasR* was downregulated by addition of
146 anhydrotetracycline (ATc) to the culture medium, thus leading to protein depletion.
147 However, we were not able to detect any growth defect after addition of ATc,
148 suggesting that *fasR* was not essential for *M. tuberculosis* survival. This result
149 prompted us to try to obtain a *fasR* knockout (KO) mutant strain by replacing the
150 *fasR* complementing plasmid with the empty vector pND255 (Fig 1C). Consistent
151 with the ability of the conditional mutant to grow in the non-permissive condition,
152 plenty of colonies were obtained in the presence of Hyg, and the replacement was
153 successfully confirmed by colony PCR (S1A Fig). We selected two Hyg-resistant
154 clones and confirmed the depletion of FasR by Western blot using total protein
155 extracts (S1B Fig). The genotype of this strain was further analyzed by Southern
156 Blot (Fig 1D), thus validating the genomic deletion of *fasR* and the generation of
157 the *fasR* KO mutant strain, named *Mtb*Δ*fasR*.
158 Once the non-essentiality of *fasR* for *M. tuberculosis* survival was confirmed, we
159 then hypothesized that deletion of this transcriptional regulator could be deleterious
160 for bacterial growth under specific conditions. In particular, we analyzed the growth
161 of *Mtb*Δ*fasR* mutant using different culture media. As shown in Fig 2, growth of
162 *Mtb*Δ*fasR* in complete 7H9 medium (7H9 + OADC) was similar to that of the wild
163 type and the complemented strain (*Mtb*Δ*fasR*-c*fasR* grown without ATc), although
164 the KO mutant reached stationary phase earlier and at lower OD_{600}. Interestingly, if
165 the medium was not supplemented with oleate and BSA (i.e. 7H9 without OADC),
166 growth defects appeared to be more pronounced, suggesting that the presence of
167 lipids in complete 7H9 medium could partially rescue the absence of FasR.
168 Moreover, *Mtb*Δ*fasR* mutant showed severe growth defects in Sauton minimal

169 medium, reaching a maximal OD_{600} of 0.3 (Fig 2). Altogether, these experiments
170 showed that FasR is not essential for *M. tuberculosis* survival, although it is
171 required for optimal bacterial growth, especially under lipid-limited conditions.
172
173 **FasR is a transcriptional activator of the *fas-acpS* operon in *M. tuberculosis***
174 We have previously demonstrated that FasR is a transcriptional activator of *fas* in
175 *M. smegmatis* [12]. Thus, to validate the role of FasR in fatty acid biosynthesis in
176 *M. tuberculosis*, we analyzed expression of the *fas-acpS* operon genes in
177 *Mtb*Δ*fasR* and in the complemented strain *Mtb*Δ*fasR*-c*fasR*. The relative amounts
178 of *fas* and *acpS* mRNAs were measured by quantitative RT-PCR after 8 days of
179 growth in complete 7H9 medium and compared to those of *Mtb*H37Rv wild type
180 strain. As shown in Fig 3, transcription of *fas* and *acpS* was reduced by 70 % and
181 40 % respectively when cells were deprived of FasR, confirming that FasR is a
182 transcriptional activator of the *fas-acpS* operon in *M. tuberculosis*.
183
184 ***fasR* knockout strongly impacts composition of *M. tuberculosis* cell envelope**
185 Previous characterization of *M. smegmatis fasR* [12] and *fas* [15] conditional
186 mutant strains revealed that reduced FAS I levels had a strong impact on fatty acid
187 and phospholipid biosynthesis. Interestingly, MA remained being synthesized in the
188 FAS I mutant for several hours after addition of ATc (non-permissive conditions),
189 although with different abundance of the various species [15]. Considering the
190 relevance that lipids have in *M. tuberculosis* survival and virulence, the impact of
191 the absence of FasR on the global lipid profile of *M. tuberculosis* was further
192 studied. We performed comparative lipidomic analyses between *Mtb*H37Rv,

193 *Mtb*Δ*fasR* and the complemented strain. Briefly, we extracted cell-associated lipids
194 as previously described [15] and analyzed the lipid content by high-performance
195 liquid chromatography-mass spectrometry with data-dependent tandem MS
196 (HPLC-MS/MS).
197 As illustrated in Fig 4, lipid analysis in the negative mode indicated that the relative
198 abundance (expressed as percentage of lipid MS signals) of phospholipids (PL)
199 and MA in the wild type and complemented strains was approximately 75 and 25
200 %, respectively. These values changed to 50 % for both PL and MA in the *fasR*
201 mutant strain, reflecting the strong impact that lower levels of *de novo* fatty acid
202 biosynthesis had in PL and MA relative abundance. The relative composition of PL
203 also showed a biased effect towards phosphatidylinositol (PI) and cardiolipins (CL),
204 which were significantly reduced in the mutant strain (Figs 4 and S2). Furthermore,
205 there was a strong reduction in the content of sulfolipids (Figs 4 and S2) and the
206 acyl chain substitutions of this lipid were consistently shorter in the mutant strain
207 (S3 Fig). A relevant change observed in the qualitative composition of the PL was
208 the significant increase in the double bonds of the acyl residues in the mutant
209 strain, with those of the CL, phosphatidylglycerol (PG) and PI being most
210 significant (S4 Fig).
211 Additionally, results obtained in the positive mode analysis showed that *M.*
212 *tuberculosis Mtb*Δ*fasR* mutant strain displayed a significant reduction in the relative
213 content of PDIM (Figs 5 and S2), with acyl substitutions that are shorter in the
214 mutant strain, compared with the wild type or the complemented strain (S3 Fig).
215 Most of the changes observed in the deletion mutant were reversed in the

216 complemented strain *Mtb*Δ*fasR*-c*fasR*, indicating that *fasR* is needed to maintain
217 the global lipid composition of *M. tuberculosis* cell envelope.
218

219 **FasR is required for *M. tuberculosis* replication in macrophages**

220 To investigate whether FasR is required for the intracellular survival of *M.*
221 *tuberculosis* in macrophages, we infected THP-1-derived macrophages with
222 exponentially growing cultures of *Mtb*H37Rv, *Mtb*Δ*fasR* and the complemented
223 strain *Mtb*Δ*fasR*-c*fasR*. To quantify bacterial uptake and intracellular replication,
224 we determined the numbers of intracellular viable bacteria at different time points
225 post-infection. As shown in Fig 6, infection with similar numbers of bacteria of each
226 strain resulted in recovery of similar numbers of CFU for all of the strains at 24 and
227 48 h post-infection. However, 120 and 144 h after the infection, intracellular
228 bacterial replication of *Mtb*Δ*fasR* strain was significantly reduced compared to that
229 of the wild type strain. The wild type phenotype was partially restored in the
230 *Mtb*Δ*fasR*-c*fasR* complemented strain at day 5 (120 h) and completely restored at
231 day 6 (144 h), indicating that the intracellular growth defect was due to the deletion
232 of *fasR* and that this regulator is necessary for optimal intracellular multiplication of
233 *M. tuberculosis* in macrophages.
234

235 **FasR regulates phagosome maturation in macrophages**

236 We have shown that the absence of FasR, and consequently reduced levels of *fas-*
237 *acpS*, have a strong impact on the composition of *M. tuberculosis* cell envelope,
238 and also on bacterial multiplication within macrophages. We hypothesized that the
239 altered bacterial cell envelope of the *Mtb*Δ*fasR* mutant may affect *M. tuberculosis*-

240 driven phagosome maturation during infection. To investigate this, we analyzed the
241 acidification of *M. tuberculosis Mtb*Δ*fasR* phagosome during infection of human
242 macrophages by staining with Lysotracker dye and measuring the phagosomal
243 acquisition of LAMP-3 (late endosomal/lysosomal markers). Interestingly, while
244 *Mtb*H37Rv prevented phagosome acidification, *Mtb*Δ*fasR* mutant strain resided in
245 phagosomes that were strongly stained by Lysotracker dye and that acquired
246 LAMP-3, suggesting that this strain cannot avoid phagosomal maturation. The
247 observed mutant phenotype was rescued in the *Mtb*Δ*fasR*-c*fasR* complemented
248 strain, indicating that the increased phagosome acidification was due to the
249 absence of FasR (Fig 7).
250

251 **Disruption of lipid homeostasis attenuates mycobacterial virulence in mice**

252 To characterize the role of FasR in an experimental model of infection, three
253 groups of BALB/c mice (10 per group) were infected intratracheally with 10^2 CFU of
254 *Mtb*H37Rv, *Mtb*Δ*fasR* and *Mtb*Δ*fasR*-c*fasR* strains. Mice were killed 60 days post-
255 infection and bacterial loads in lungs were determined. CFU counts were
256 significantly reduced for the *Mtb*Δ*fasR* strain compared to *Mtb*H37Rv, while the
257 wild type phenotype was restored in the *Mtb*Δ*fasR*-c*fasR* strain (Fig 8), indicating
258 that FasR is essential for survival and multiplication of *M. tuberculosis* in mice.
259

260 ## Discussion

261

262 In a previous investigation we identified FasR, a TetR-like transcriptional regulator
263 that specifically binds to the *fas* promoter region to activate its expression, and
264 found that FasR was essential for *in vitro* growth of *M. smegmatis* [12]. However,
265 its role in *M. tuberculosis* viability was controversial. Using Himar 1 transposon
266 mutagenesis it was initially proposed that FasR was essential for *M. tuberculosis*
267 survival [16,17]. However, more recently, De Jesus *et al* found that FasR was
268 dispensable for growth, by assessing the composition of a highly saturated library
269 of transposon mutants *of M. tuberculosis* by deep sequencing [18]. Moreover, the
270 relevance of FasR for mycobacterial survival in intracellular environments or animal
271 models had not been investigated. In this work, by constructing a deletion *fasR*
272 mutant and a complemented strain, we unequivocally established that FasR is not
273 essential for *M. tuberculosis* viability, although it is required for optimal growth of *M.*
274 *tuberculosis in vitro* and for virulence in macrophages and mice model of infection.
275 We had shown that FasR binds to three inverted repeats present in the promoter
276 region of the *fas-acpS* operon thereby activating fatty acid biosynthesis in *M.*
277 *smegmatis* [12]. Furthermore, we also demonstrated, *in vitro* and *in vivo,* that FasR
278 binding to its target promoter is regulated by long-chain acyl-CoAs, the main
279 products of FAS I [12]. The *fas* and *acpS* genes form a bicistronic operon, coding
280 for the FAS I synthase and the 4-phosphopantetheinyl transferase, respectively;
281 the latter being an essential enzyme to produce functional acyl carrier protein (holo
282 ACP), central to all fatty-acid biosynthesis systems. Transcriptional studies carried
283 out in this work showed that expression of the *fas-acpS* operon genes in *M.*
284 *tuberculosis* Δ*fasR* was reduced by 70 % and 40 %, respectively (Fig 3). This
285 result confirmed that FasR is a transcriptional activator of the *fas-acpS* operon in

286 *M. tuberculosis*. The activator nature of FasR highlights a remarkable difference
287 with most transcriptional regulators of fatty acid biosynthesis, which are repressor
288 proteins [19]. Moreover, FasR is a member of the TetR family of regulators, and
289 the vast majority of these proteins are transcriptional repressors, with very few
290 acting as activators [20].
291 Since fatty acids are major constituents not only of phospholipids but also of
292 several complex lipids, inactivation of FasR was expected to modify synthesis of
293 several components of the cell envelope essential for mycobacterial viability and/or
294 virulence. Indeed, lipidomic analysis of *Mtb*Δ*fasR* and comparison with wild type
295 and complemented strains proved this hypothesis. As expected, reduced levels of
296 fatty acid biosynthesis in *Mtb*Δ*fasR* had a strong impact on relative abundance of
297 phospholipids and their relative and qualitative composition (Figs 4 and S2).
298 Phosphatidylinositol (PI) and cardiolipins (CL) were significantly reduced in the
299 mutant strain, while the acyl chains present in and these phospholipids exhibited a
300 significant increase in their double bond content (S4 Fig). Mycobacterial
301 phospholipids have been implicated in immunomodulation. For example, CL is
302 processed into lysocardiolipin by the lysosomal phospholipase A2 during infection,
303 probably generating active lipid derivatives that play important roles during
304 infection or persistence within the host [21]. The *Mtb*Δ*fasR* mutant strain also
305 displayed a strong reduction in the content of sulfolipids (Figs 4 and S2) and PDIM
306 (Figs 5 and S2). Interestingly, the acyl chain substitutions of both lipids were
307 consistently shorter compared to the wild type *Mtb*H37Rv strain (S3 Fig). On this
308 regard, a *M. tuberculosis* mutant strain deficient in sulfolipids and PDIM has been
309 shown to be attenuated in macrophages and in mice models of infection [8].

310 Moreover, during infection, genes involved in the biosynthesis of sulfolipids and
311 PDIM are upregulated [22,23] and the mass of these lipids increases [24,25].
312 Altogether, our results showed that *M. tuberculosis fasR* mutant exhibits an
313 extensive rearrangement of the lipid components of the cell envelope, that are
314 reversed in the complemented strain *Mtb*Δ*fasR*-c*fasR*, confirming that FasR is
315 needed to maintain the lipid homeostasis of the *M. tuberculosis* cell envelope. As
316 the mycobacterial cell envelope is the interface with the host, FasR modulation of
317 its structure and consequent responsiveness to immune factors might be important
318 in determining the state of an infection.
319 Consistent with this hypothesis, we have shown that FasR is necessary for optimal
320 intracellular multiplication of *M. tuberculosis* in macrophages, therefore confirming
321 the role of cell wall components in the ability of the pathogen to survive and
322 multiply intracellularly [26]. Persistence of the tubercle bacillus inside cells relies
323 upon inhibition of phagosome maturation and acidification [27]. In this context,
324 several cell wall lipids have been shown to modulate host endocytic pathways. This
325 is the case for Man-Lam, TDM, PIM and PDIM, which, besides their role in
326 phagocytosis, also mediate intracellular trafficking and vacuole maturation arrest
327 induced by *M. tuberculosis* [8]. More recently, PDIM and SL were shown to be
328 involved in controlling autophagy-related pathways in human macrophages [28].
329 Considering the changes observed in the PDIM content of the *Mtb*Δ*fasR* mutant,
330 we analyzed the acidification of phagosome during infection of human
331 macrophages. Interestingly, while the wild type *Mtb*H37Rv and the complemented
332 strains prevented phagosome acidification, the *Mtb*Δ*fasR* mutant was impaired in
333 avoiding phagosomal maturation, clearly indicating that increased phagosome

334 acidification was due to absence of FasR (Fig 7). These results suggested that
335 although FasR is not essential for *in vitro* growth, regulation of lipid biosynthesis,
336 mediated by FasR, is critical for macrophage infection. Moreover, using a mouse
337 model of infection we demonstrated the essentiality of FasR for *M. tuberculosis*
338 virulence *in vivo* (Fig 8), most probably as a consequence of the loss of various
339 mycobacterial lipids that contribute to pathogenicity.
340 Co-evolution with the human immune system prompted *M. tuberculosis* to generate
341 exquisite mechanisms of immunomodulation and immune evasion, many of which
342 depend on its cell envelope. In fact, comparison of cell envelope components
343 between *M. tuberculosis* and ancestral species revealed a restructuring of the
344 mycomembrane glycolipid components, including mycolic acids and free lipids of
345 the outer leaflet [11]. The observed phenotype of the FasR mutant is probably a
346 consequence of additive effects, as several components of the cell envelope were
347 altered. *M. tuberculosis* interferes with innate immune signalling pathways, for
348 example by masking pathogen-associated molecular patterns with PDIM [29] and
349 inhibiting toll-like receptor 2 with sulfoglycolipids [30]. PDIM is also crucial for other
350 steps of infection: it contributes to cell envelope properties, such as the
351 permeability barrier [31], improves the invasiveness of *M. tuberculosis* and its
352 capacity to arrest phagosome maturation, possibly by inducing changes in the
353 plasma membranes of human macrophages during infection [32], and directly
354 protects against reactive nitrogen species [33]. Therefore, reduced content of these
355 molecules (and/or changes in their chemical composition) may contribute to
356 sensitivity to the bactericidal activities of phagocytes.

357 Altogether, our data indicate an important role for FasR in *M. tuberculosis*
358 pathogenesis and encourage further investigations into the contribution of lipid
359 regulation to virulence. It is well known that *M. tuberculosis* is able to modulate the
360 expression of its cell wall components in response to environmental changes,
361 however, little is known about their reorganization during infection, and to a lesser
362 extent about the regulatory mechanisms involved in this process [11]. The
363 dynamism of the bacterial cell envelope should be a tightly regulated phenomenon,
364 ensuring *M. tuberculosis* survival during infection. Thus, specific regulatory
365 components involved in this process, as we have demonstrated for FasR, would
366 constitute interesting targets for the development of new treatment strategies.
367 Along this line of thinking, we recently solved the crystal structures of *M.*
368 *tuberculosis* FasR in complex with DNA and the acyl effector ligands, which
369 provided insights into the molecular sensory and transmission mechanisms of this
370 regulatory protein [34]. This knowledge could lead now to perform structure-guided
371 drug discovery strategies to identify anti-mycobacterial molecules with novel
372 mechanisms of action.
373

374 ## Materials and methods

375

376 **Ethics statement**

377 All animal experiments were performed in compliance with the regulations of the
378 Institutional Animal Care and Use Committee (CICUAE) of INTA with the
379 authorization Number 20/2016.

380

381 **Bacterial strains, culture and transformation conditions**

382 The *E. coli* strain DH5α [35] was used for routine subcloning and was transformed
383 according to Sambrook *et al.* [36]. *M. tuberculosis* H37Rv [37], *Mtb*Δ*fasR* and
384 *Mtb*Δ*fasR*-c*fasR* were grown at 37 ºC in Middlebrook 7H9 broth (DIFCO)
385 supplemented with 0.2 % glycerol, 0.03 % Tyloxapol and 10 % OADC or
386 Middlebrook 7H10 agar (DIFCO) supplemented with 0.2 % glycerol and 10 %
387 OADC. Hygromycin (Hyg, 50 µg/ml), kanamycin (Kan, 15 µg/ml) and streptomycin
388 (Str, 12 µg/ml) were added when needed.

389 Recombinant plasmids and strain genotypes are listed in electronic supplementary
390 material (S1 and S2 Tables).

391

392 **DNA manipulation, plasmid construction and mutant generation**

393 Isolation of plasmid DNA, restriction enzyme digestion and agarose gel
394 electrophoresis were carried out by conventional methods [36]. Genomic DNA of
395 *M. tuberculosis* was obtained as described previously [38]. For plasmid generation
396 purposes, all PCR products were ligated into the pCR®-Blunt II-TOPO® Vector
397 (Invitrogen) according to the manufacturer's recommendation.

398 For the construction of the *fasR* mutant allele, a fragment of 946 bp containing 58
399 bp of the *fasR* 5´end plus 882 bp of the upstream region was PCR amplified from
400 genomic DNA using oligonucleotides 3208_1up and 3208_2down (S3 Table). The
401 PCR product was cloned in the pCR BluntII TOPO vector (Invitrogen). The
402 resulting plasmid was digested first with *Eco*RV and after with *Xho*I/*Nde*I. The 940

403 bp fragment obtained was cloned in the suicide vector pJG1100 [39,40] digested
404 with the same enzymes, generating plasmid pFR34. Additionally, a fragment of 883
405 bp containing 87 bp of the *fasR* 3´end plus 784 bp of the downstream region was
406 PCR amplified from genomic DNA using oligonucleotides 3208_3up and
407 3208_4down (S3 Table). The PCR product was cloned in the pCR BluntII TOPO
408 vector (Invitrogen). The resulting plasmid was digested first with *Eco*RI and after
409 with *Nde*I/*Spe*I and the fragment (877 bp) was cloned in pFR34 vector digested
410 with the same enzymes, generating plasmid pFR35.
411 For the construction of a *fasR* merodiploid strain, the fragment resulting from the
412 digestion of the plasmid pFR3 [12] with *Xba*I and *Eco*RI was cloned between the
413 *Avr*II and *Mfe*I sites in plasmid pGA44 [41]. The resulting plasmid, pFR33, is an
414 integrative plasmid that harbours *fasR* expressed under the control of *Ptr* promoter
415 and the TetR/Pip OFF system necessary for its regulation.
416 Deletion of *fasR* was accomplished by homologous recombination. After
417 transformation of *M. tuberculosis* with plasmid pFR35, the first recombination event
418 was selected on 7H10 medium containing Kan and Hyg and resistant colonies
419 were screened by colony PCR. The merodiploid strain was generated by
420 integration of pFR33 at the L5 *attB* site and transformants were plated on 7H10
421 with Hyg, Kan and Str. Deletion of the wild type gene by allelic replacement was
422 accomplished by plating bacteria on 7H10 agar plates supplemented with Str and
423 2.5 % sucrose. The Hyg^s, Kan^s, Str^r, $Sucrose^r$ colonies were tested by PCR and
424 the *fasR* conditional knockdown strain was named *Mtb*Δ*fasR*-c*fasR*. Generation of
425 a *fasR* knockout strain (*Mtb*Δ*fasR*) was obtained by swapping the pFR33 plasmid
426 at the L5 *attB* site with the pND255 plasmid. Transformants were selected on 7H10

427 plates containing Hyg. Deletion of *fasR* was confirmed by Southern Blot and colony
428 PCR.

429 **Southern Blot**

430 10 µg of genomic *M. tuberculosis* DNA was digested overnight with an excess of
431 *Xho*I, and the fragments were separated by electrophoresis in a 0.7% agarose gel.
432 Southern blotting was carried out using Hybond-N^+ membrane (Amersham) and
433 DIG High Prime DNA Labeling and Detection Starter kit II (Roche), following the
434 indications of the manufacturer. The probe consisted of a 594 bp fragment
435 amplified with oligonucleotides Southern_1fasRTB and Southern_2fasRTB (S3
436 Table), corresponding to the upstream genomic region of *fasR*.

437 **Western blot**

438 Equal amounts of protein extracts were loaded on 4-12 % NuPAGE gels
439 (Invitrogen) and transferred onto nitrocellulose membranes using a dry
440 electrophoresis transfer apparatus (Invitrogen). Membranes were incubated in
441 TBS-Tween blocking buffer (20 mM Tris pH 7.5, 150 mM NaCl, 0.1 % Tween 20)
442 with 5 % (w/v) skimmed milk powder for 2 h at 4 ºC prior to overnight incubation
443 with 1:1000 dilution of monoclonal anti-FasR primary antibody (Alere™).
444 Membranes were washed in TBS-Tween three times at room temperature, and
445 then incubated with 1:100000 secondary antibody Anti-Mouse Kappa conjugated to
446 Horseradish Peroxidase (Southern Biotech) for 2 h before washing again. Signals
447 were detected using Chemiluminescent Peroxidase Substrate (Sigma-Aldrich).
448 Monoclonal mouse anti-RpoB antibodies were purchased from NeoClone and used
449 1:20000.

450

451 **RNA techniques**

452 RNA was extracted from *M. tuberculosis* strains grown for 8 days in complete 7H9
453 media using Trizol-phenol based methods [41] and treated, when needed, with
454 RQ1 RNase-Free DNase (Promega). qRT-PCR was performed using second
455 strand cDNA as the template, generated with SuperScript III Reverse
456 Transcriptase (Invitrogen), random primers and a green fluorochrome as the
457 indicator dye (qPCR master mix, Biodynamics). The expression of *fas*, *fasR* and
458 *acpS* was quantified after normalization of RNA levels to the expression of the *sigA*
459 gene as previously described [15]. qPCR data are presented as relative expression
460 values normalized to *sigA* and to the wild type strain H37Rv. qPCR cycling
461 conditions were as follows: 95 ºC for 2 min followed by 40 cycles of 95 ºC for 15 s,
462 58 ºC for 15 s and 68 ºC for 20 s. The sequences of all the primers used are listed
463 in electronic supplementary material (S3 Table).

464

465 **Lipid analysis**

466 Cell-associated lipid for lipidomic analyses were prepared as previously described
467 [15]. Briefly, cell pellets of cultures grown at 37 ºC in Middlebrook 7H9 broth
468 (DIFCO) supplemented with 0.2 % glycerol, 0.03 % Tyloxapol and 10 % OADC
469 were washed with 50 mM ammonium acetate, pH 7.8 and transferred to glass
470 tubes containing 5 ml $CHCl_3$:CH_3OH (2:1, v/v). Samples were incubated overnight
471 at 4 ºC with gentle agitation. After centrifugation, bacterial pellets were subjected to
472 an additional extraction using $CHCl_3$:CH_3OH (1:2, v/v) for 2 h. Organic extracts
473 were pooled and dried under nitrogen at 4 ºC. Lipids were resuspended in 3 ml of
474 $CHCl_3$, washed with 3 ml of H_2O and the organic phase was transferred to pre-

475 weighted glass tubes, dried under nitrogen at 4 ºC and re-weighted on a
476 microbalance. Extracts were dissolved in $CHCl_3$:CH_3OH (1:1, v/v) at 1 mg ml^{-1} and
477 centrifuged at 3000 g for 5 min. Lipids were analyzed in an Agilent 1200 series
478 HPLC system with a Reprospher (Dr Maish) 100 C8 column (1.8 µm, 50 mm
479 length, 2 mm ID). The flow rate was 0.3 ml min^{-1} in binary gradient mode with the
480 following elution program: the column was equilibrated with 100 % mobile phase A
481 [CH_3OH:H_2O (99:1, v/v), containing 0.05 mM $AcNH_4$]. 2 µl of each sample were
482 injected, and the same elution conditions continued for 1 min, followed by a 12 min
483 gradient to 100 % mobile phase B [isopropanol:hexane:H_2O (79:20:1, v/v),
484 containing 0.05 mM $AcNH_4$], finally holding this condition for 1 min. The column
485 was equilibrated for 2 min with 100 % mobile phase A before injection of the next
486 sample. An Agilent 6500 series Q-TOF instrument with a Dual AJS ESI was used
487 for mass analysis. Ionization gas temperature was maintained at 200 ºC with a 14 l
488 min^{-1} drying gas flow, a 35 psig nebulizer pressure and 3500 Volts. Spectra were
489 collected in positive and negative mode from *m/z* 115 to 3000 at 4 spectra s^{-1}.
490 Automatic tandem-MS (MS-MS) was obtained in data-dependent acquisition mode
491 at 15 MS-MS per cycle. Continuous infusion calibrants included *m/z* 121.051 and
492 922.010 in positive-ion mode and *m/z* 119.035 and 955.972 in negative-ion mode.
493 CID-MS was carried out with an energy of 50 volts. For the comparative analysis,
494 the column is conditioned by four successive mock injections before randomized
495 QCs and mycobacterial samples are analyzed. Lipid features were annotated
496 based on structural MS-MS information. Lipid classes' retention times (RT) were

497 identified using characteristics fragmentation patterns [42]. Individual molecules in
498 each class were then identified based on exact mass and RT.
499
500 **Colony-forming units (CFU) analysis**
501 *M. tuberculosis* H37Rv, *Mtb*Δ*fasR* and *Mtb*Δ*fasR*-c*fasR* strains were used to infect
502 THP-1 cells (MOI=5). The day before infection $4x10^5$ THP-1 cells were plated in a
503 24-well plate in RPMI Medium with 4.5 g/L glucose, 10 % heat inactivated fetal calf
504 serum (Internegocios) and 2 mM L-glutamine (full medium) plus 50 nM phorbol 12-
505 myristate 13-acetate (PMA) to allow differentiation of the cells to macrophages. On
506 the infection day, cells were washed and a suspension of the different strains of *M.*
507 *tuberculosis* in RPMI medium was added. After 2 h of uptake, cells were washed 3
508 times with PBS and fresh full RPMI medium plus gentamicin 10 µg mL^{-1} was
509 added. Cells were incubated at 37 °C in 5 % CO_2 atmosphere. Subsequently, at
510 the indicated time points, cells were lysed in sterile water and serially diluted in
511 PBS-Tween 80 0.05 %. Dilutions were plated on Middlebrook 7H10 complete agar
512 medium (Difco Laboratories). Colonies were counted after 3 to 4 weeks to
513 determine CFU.
514
515 **Mouse infections**
516 Bacillary suspensions of the different strains were adjusted to 100 viable cells in
517 100 ml phosphate buffer saline (PBS). Each animal was anesthetized and
518 intratracheally inoculated with *M. tuberculosis* strains (*Mtb*H37Rv, *Mtb*Δ*fasR* and
519 *Mtb*Δ*fasR*-c*fasR*). Infected mice were kept in cages fitted with microisolators
520 connected to negative pressure. Groups of 10 mice were infected with the different

521 *M. tuberculosis* strains. The inoculum doses were determined by enumerating CFU
522 recovered from the lungs of three mice per strain, 24 h post-infection. Seven mice
523 per group were killed at 60 days after infection and lungs removed and
524 homogenized. Four dilutions of each homogenate were spread onto triplicate
525 plates of Middlebrook 7H10 complete agar medium. The number of colonies was
526 counted after 3 to 4 weeks.
527

528 **Infection of THP-1 cells and indirect immunofluorescence (IFI)**

529 *M. tuberculosis* strains were covalently stained with FITC (Sigma-Aldrich). Briefly,
530 1×10^9 bacteria were washed twice with 0.1 M PBS and suspended in 1 ml of the
531 same solution. FITC was added to a final concentration of 5 µg/ml and incubated in
532 the dark for 1 h at 37 °C. Bacteria were washed gently with PBS until
533 unincorporated dye was eliminated, and then were used to infect THP-1 cells.
534 THP-1 cells were maintained in complete full RPMI medium. The day before
535 infection $2x10^5$ THP-1 cells per well were plated in a 24-well plate with coverslips in
536 full RPMI medium plus 50 nM PMA to allow differentiation of the cells to
537 macrophages. On the day of infection, cells were washed and infected with the
538 different stained *M. tuberculosis* strains (*Mtb*H37Rv, *Mtb*Δ*fasR* and *Mtb*Δ*fasR*-
539 c*fasR*) prepared in RPMI medium, at a MOI of 5. After 2 h of uptake, cells were
540 washed and incubated with 10 μM Lysotracker Red DND-99 for 1 hour to allow the
541 staining of acidic compartments, fixed with 4 % paraformaldehyde solution in PBS
542 for 30 min and subjected to immunofluorescence analysis.

543 Cells were quenched by incubation with 50 mM NH_4Cl solution in PBS for 30 min.
544 and permeabilized with 0.05 % saponin/1 % BSA in PBS for 15 min, followed by
545 overnight incubation with goat anti-LAMP-3 (Santa Cruz Biotechnology, Santa
546 Cruz, CA) primary antibody diluted 1:50 in PBS. Secondary anti-goat antibody
547 conjugated to Cy3 (Jackson Immuno Research Labs, Inc.) was diluted 1:600 in
548 PBS. Cells were mounted with mounting medium (Dako, Denmark) and analysed
549 by confocal microscopy using an SP5 AOBS confocal microscope (Leica
550 Microsystems, Germany). Mycobacterial internalization was monitored by following
551 FITC fluorescence (green). Lysotracker Red DND-99 or LAMP-3 association with
552 mycobacterial phagosomes was analysed in at least 250 cells using Fiji software
553 (U.S. National Institutes of Health, Bethesda, MD) as described previously [43].
554 The experiments were performed in duplicates in three independent experiments.
555 The statistical analysis was performed using two-tailed Student's t-test.
556

557 ## References

558 1. WHO. Global tuberculosis report. 2019.
559 2. Chiaradia L, Lefebvre C, Parra J, Marcoux J, Burlet-Schiltz O, Etienne G, et
560 al. Dissecting the mycobacterial cell envelope and defining the composition
561 of the native mycomembrane. Sci Rep. 2017;7: 12807. doi:10.1038/s41598-
562 017-12718-4
563 3. Daffé M, Marrakchi H. Unraveling the Structure of the Mycobacterial
564 Envelope. Microbiol Spectr. 2019;7: GPP3-0027–2018.
565 doi:10.1128/microbiolspec.GPP3-0027-2018.Correspondence

566 4. Brennan PJ, Nikaido H. The envelope of mycobacteria. AnnuRevBiochem.
567 1995;64: 29–63.
568 5. Daffe M, Reyrat JM. The Mycobacterial Cell Envelope. Daffé M, Reyrat JM,
569 editors. ASM Press; 2008.
570 6. Russell DG, Barry CE, Flynn JL. Tuberculosis: What We Don't Know Can,
571 and Does, Hurt Us. Science (80-). 2010;328: 852–856.
572 doi:10.1126/science.1184784
573 7. Neyrolles O, Guilhot C. Recent advances in deciphering the contribution of
574 Mycobacterium tuberculosis lipids to pathogenesis. Tuberculosis. 2011;91:
575 187–195. doi:10.1016/j.tube.2011.01.002
576 8. Passemar C, Arbues A, Malaga W, Mercier I, Moreau F, Lepourry L, et al.
577 Multiple deletions in the polyketide synthase gene repertoire of
578 mycobacterium tuberculosis reveal functional overlap of cell envelope lipids
579 in host-pathogen interactions. Cell Microbiol. 2014;16: 195–213.
580 doi:10.1111/cmi.12214
581 9. Vromman F, Subtil A. Exploitation of host lipids by bacteria. Curr Opin
582 Microbiol. 2014;17: 38–45. doi:10.1016/j.mib.2013.11.003
583 10. Teng O, En Ang CK, Guan XL. Macrophage-bacteria interactions-A lipid-
584 centric relationship. Front Immunol. 2017;8. doi:10.3389/fimmu.2017.01836
585 11. Dulberger C, Rubin E, Boutte CC. The mycobacterial cell envelope — a
586 moving target. Nat Rev Microbiol. 2020;18: 47–59. doi:10.1038/s41579-019-
587 0273-7
588 12. Mondino S, Gago G, Gramajo H. Transcriptional regulation of fatty acid
589 biosynthesis in mycobacteria. Mol Microbiol. 2013;89: 372–387.

590 13. Salzman V, Mondino S, Sala C, Cole ST, Gago G, Gramajo H.
591 Transcriptional regulation of lipid homeostasis in mycobacteria. Mol
592 Microbiol. 2010;78: 64–77.
593 14. Boldrin F, Casonato S, Dainese E, Sala C, Dhar N, Palù G, et al.
594 Development of a repressible mycobacterial promoter system based on two
595 transcriptional repressors. Nucleic Acids Res. 2010;38: 1–11.
596 doi:10.1093/nar/gkq235
597 15. Cabruja M, Mondino S, Tsai YT, Lara J, Gramajo H, Gago G. A conditional
598 mutant of the fatty acid synthase unveils unexpected cross talks in
599 mycobacterial lipid metabolism. Open Biol. 2017;7.
600 16. Sassetti CM, Boyd DH, Rubin EJ. Genes required for mycobacterial growth
601 defined by high density mutagenesis. MolMicrobiol. 2003;48: 77–84.
602 17. Griffin JE, Gawronski JD, DeJesus MA, Ioerger TR, Akerley BJ, Sassetti CM.
603 High-resolution phenotypic profiling defines genes essential for
604 mycobacterial growth and cholesterol catabolism. PLoS Pathog. 2011;7: 1–9.
605 doi:10.1371/journal.ppat.1002251
606 18. DeJesus MA, Gerrick ER, Xu W, Park SW, Long JE, Boutte CC, et al.
607 Comprehensive Essentiality Analysis of the Mycobacterium tuberculosis
608 Genome via sturating transposon mutagenesis. MBio. 2017;8:e02133–1.
609 doi:10.1128/mBio.02133-16
610 19. Zhu K, Zhang YM, Rock CO. Transcriptional regulation of membrane lipid
611 homeostasis in Escherichia coli. JBiolChem. 2009;284: 34880–34888.
612 20. Cuthbertson L, Nodwell JR. The TetR Family of Regulators. Microbiol Mol
613 Biol Rev. 2013;77: 440–475. doi:10.1128/mmbr.00018-13

614 21. Fischer K, Chatterjee D, Torrelles J, Brennan PJ, Kaufmann SHE, Schaible
615 UE. Mycobacterial Lysocardiolipin Is Exported from Phagosomes upon
616 Cleavage of Cardiolipin by a Macrophage-Derived Lysosomal Phospholipase
617 A 2 . J Immunol. 2001;167: 2187–2192. doi:10.4049/jimmunol.167.4.2187
618 22. Graham JE, Clark-Curtiss JE. Identification of Mycobacterium tuberculosis
619 RNAs synthesized in response to phagocytosis by human macrophages by
620 selective capture of transcribed sequences (SCOTS). Proc Natl Acad Sci.
621 1999;96: 11554–11559.
622 23. Rodríguez JE, Ramírez AS, Salas LP, Helguera-Repetto C, Gonzalez-y-
623 Merchand J, Soto CY, et al. Transcription of Genes Involved in Sulfolipid and
624 Polyacyltrehalose Biosynthesis of Mycobacterium tuberculosis in
625 Experimental Latent Tuberculosis Infection. PLoS One. 2013;8.
626 doi:10.1371/journal.pone.0058378
627 24. Griffin JE, Pandey AK, Gilmore SA, Mizrahi V, Mckinney JD, Bertozzi CR, et
628 al. Cholesterol catabolism by Mycobacterium tuberculosis requires
629 transcriptional and metabolic adaptations. Chem Biol. 2012;19: 218–227.
630 doi:10.1038/jid.2014.371
631 25. Yang X, Nesbitt NM, Dubnau E, Smith I, Sampson NS. Cholesterol
632 Metabolism Increases the Metabolic Pool of Propionate in M. tuberculosis.
633 Biochemistry. 2009;48: 3819–3821. doi:10.1021/bi9005418.Cholesterol
634 26. Garcia-Vilanova A, Chan J, Torrelles JB. Underestimated Manipulative Roles
635 of Mycobacterium tuberculosis Cell Envelope Glycolipids During Infection.
636 Front Immunol. 2019;10. doi:10.3389/fimmu.2019.02909
637 27. Rohde K, Yates RM, Purdy GE, Russell DG. Mycobacterium tuberculosis

638 and the environment within the phagosome. Immunol Rev. 2007;219: 37–54.
639 28. Bah A, Sanicas M, Nigou J, Guilhot C, Astarie-Dequeker C, Vergne I. The
640 Lipid Virulence Factors of Mycobacterium tuberculosis Exert Multilayered
641 Control over Autophagy-Related Pathways in Infected Human Macrophages.
642 Cells. 2020;9: 666. doi:10.3390/cells9030666
643 29. Cambier CJ., Takaki KK., Larson RP., Hernandez RE., Tobin DM., Urdahl
644 KB., et al. Mycobacteria manipulate macrophage recruitment through
645 coordinated use of membrane lipids. Nature. 2014;505: 218–222.
646 doi:10.1038/nature12799
647 30. Blanc L, Gilleron M, Prandi J, Song O, Jang M, Gicquel B, et al.
648 Mycobacterium tuberculosis inhibits human innate immune responses via the
649 production of TLR2 antagonist glycolipids. Proc Natl Acad Sci. 2017;114:
650 11205–11210. doi:10.1073/pnas.1707840114
651 31. Camacho LR, Constant P, Raynaud C, Lane M, Triccas JA, Gicquel B, et al.
652 Analysis of the Phthiocerol Dimycocerosate Locus of Mycobacterium
653 tuberculosis. J Biol Chem. 2001;276: 19845–19854.
654 doi:10.1074/jbc.M100662200
655 32. Astarie-Dequeker C, Le Guyader L, Malaga W, Seaphanh FK, Chalut C,
656 Lopez A, et al. Phthiocerol dimycocerosates of M. tuberculosis participate in
657 macrophage invasion by inducing changes in the organization of plasma
658 membrane lipids. PLoS Pathog. 2009;5: e1000289.
659 doi:10.1371/journal.ppat.1000289
660 33. Rousseau C, Winter N, Pivert E, Bordat Y, Neyrolles O, Avé P, et al.
661 Production of phthiocerol dimycocerosates protects Mycobacterium

662 tuberculosis from the cidal activity of reactive nitrogen intermediates
663 produced by macrophages and modulates the early immune response to
664 infection. Cell Microbiol. 2004;6: 277–287. doi:10.1111/j.1462-
665 5822.2004.00368.x
666 34. Lara J, Diacovich L, Trajtenberg F, Larrieux N, Malchiodi EL, Fernandez M,
667 et al. Mycobacterium tuberculosis FasR senses long fatty acyl-CoA through a
668 tunnel , inducing DNA-dissociation via a transmission spine. Available from
669 https://www.biorxiv.org/content/10.1101/2020.03.05.978833v2 doi:
670 https://doi.org/10.1101/2020.03.05.978833
671 35. Hanahan D. Studies on transformation of Escherichia coli with plasmids.
672 JMolBiol. 1983;166: 557–580.
673 36. Sambrook J. EFFTM. Molecular cloning: a laboratory manual, 2nd ed. Cold
674 Spring Harbor Laboratory Press, Cold Spring Harbor, N.Y.; 1989.
675 37. Cole ST, Brosch R, Parkhill J, Garnier T, Churcher C, Harris D, et al.
676 Deciphering the biology of Mycobacterium tuberculosis from the complete
677 genome sequence. Nature. 1998;393: 537–544.
678 38. Connell ND. Mycobacterium: isolation, maintenance, transformation, and
679 mutant selection. Methods Cell Biol. 1994;45: 107–125.
680 39. Gomez JE, Bishai WR. whmD is an essential mycobacterial gene required
681 for proper septation and cell division. Proc Natl Acad Sci U S A. 2000;97:
682 8554–8559. doi:10.1073/pnas.140225297
683 40. Muñoz-Elías EJ, McKinney JD. Carbon metabolism of intracellular bacteria.
684 Cell Microbiol. 2006;8: 10–22. doi:10.1111/j.1462-5822.2005.00648.x
685 41. Kolly GS, Boldrin F, Sala C, Dhar N, Hartkoorn RC, Ventura M, et al.

686 Assessing the essentiality of the decaprenyl-phospho-d-arabinofuranose
687 pathway in Mycobacterium tuberculosis using conditional mutants. Mol
688 Microbiol. 2014;92: 194–211. doi:10.1111/mmi.12546
689 42. Layre E, Sweet L, Hong S, Madigan CA, Desjardins D, Young D, et al. A
690 comparative lipidomics platform for chemotaxonomic analysis of
691 Mycobacterium tuberculosis. Chem Biol. 2011;23: 1537–1549.
692 doi:10.1038/jid.2014.371
693 43. Vázquez CL, Bianco MV, Blanco FC, Forrellad MA, Gutierrez MG, Bigi F.
694 Mycobacterium bovis Requires P27 (LprG) To Arrest Phagosome Maturation
695 and Replicate within Bovine Macrophages. Infect Immun. 2017;85: 1–11.
696
697
698 ## Figure captions
699
700 **Fig 1. Schematic representation of the genetic organization of the**
701 **chromosomal region of *fasR*.**
702 (**A**) Wild type H37Rv strain (*Mtb*H37Rv), (**B**) *fasR* conditional knockdown strain
703 (*Mtb*Δ*fasR*-c*fasR*) and (**C**) *fasR* KO strain (*Mtb*Δ*fasR*). (**D**) Southern Blot analysis
704 of the different strains: chromosomal DNA was digested with XhoI and probed for
705 hybridization with the probe indicated with a black bar, corresponding to the 5´ end
706 of the *Rv3207* gene.
707
708 **Fig 2. Growth of *M. tuberculosis* strains.**

709 Growth curves of the wild type strain (*Mtb*H37Rv), the *fasR* *Mtb*Δ*fasR*-c*fasR* strain
710 grown without ATc (complemented strain) and *fasR* KO strain (*Mtb*Δ*fasR*) were
711 obtained in 3 different media (7H9 complete, 7H9 without OADC and Sauton).
712 Growth was followed by measuring $OD_{600\ nm}$. Results are representative of three
713 independent experiments.
714
715 **Fig 3. Relative expression levels of *fasR*, *fas* and *acpS* mRNAs measured by**
716 **quantitative RT-PCR.**
717 Values were normalized to *sigA* and to the wild type strain (*Mtb*H37Rv). Samples
718 for RNA extraction were collected at OD_{600nm} ~ 0.3.
719
720 **Fig 4. Lipid profile in negative ion mode**
721 LC-MS analyses (negative mode) of the phospholipids and mycolic acids present
722 in the wild type strain (*Mtb*H37Rv), the *fasR* complemented strain (*Mtb*Δ*fasR*-
723 c*fasR*) and *fasR* KO strain (*Mtb*Δ*fasR*). The values indicated represent the relative
724 abundance of the MS signals corresponding to the different lipid classes found in
725 the samples. Results are the means of three independent experiments. CL,
726 cardiolipin; PI, phosphatidylinositol; PIM, phosphatidylinositol mannosides; PG,
727 phosphatidylglycerol; PE, phosphatidylethanolamine; SL, sulfolipids; MA, mycolic
728 acids.
729
730 **Fig 5. Lipid profile in positive ion mode**
731 LC-MS analyses (positive mode) of lipids present in the wild type strain
732 (*Mtb*H37Rv), the *fasR* complemented strain (*Mtb*Δ*fasR*-c*fasR*) and *fasR* KO strain

733 (*Mtb*Δ*fasR*). The values indicated represent the relative abundance of the MS
734 signals corresponding to the different lipid classes found in the samples. Results
735 are the means of three independent experiments. TAG, triacylglycerol; DAG,
736 diacylglycerol; MMDAG, monomycolyl DAG; PDIM, phthiocerol dimycocerosates;
737 GroMM, glycerol monomycolate; TMM, trehalose monomycolate.
738
739 **Fig 6. FasR is required for the intracellular survival of *M. tuberculosis*.**
740 THP-1-derived macrophages were infected with wild type *M. tuberculosis* H37Rv
741 (*Mtb*H37Rv), *fasR* mutant (*Mtb*Δ*fasR*) and the complemented *fasR* strain
742 (*Mtb*Δ*fasR*-c*fasR*) a MOI =5. At different time post-infection (24, 48, 120, 144
743 hours) cells were washed and intracellular viable bacteria were counted on agar
744 plates. Bars represent the average of three independent experiments performed in
745 triplicate wells with standard deviation.
746
747 **Fig 7. FasR regulates phagosome maturation in macrophages.**
748 Confocal microscopy analysis of THP-1 macrophages infected with wild type *M.*
749 *tuberculosis* H37Rv (*Mtb*H37Rv), *fasR* mutant (*Mtb*Δ*fasR*) and the complemented
750 *fasR* strain (*Mtb*Δ*fasR*-*cfasR*). A) Representative images of THP-1 macrophages
751 infected with the different strains labelled with FITC (green fluorescence) using a
752 MOI=5. After 2 h of uptake, cells were washed and incubated with Lysotracker Red
753 DND-99 for 1 hour to allow the staining of acidic compartments, fixed and
754 subjected to immunofluorescence. The infected and fixed cells were used to detect
755 LAMP-3 by indirect immunofluorescence using a specific antibody against LAMP-3.
756 Scale bars: 10 μm. Merge indicates the location of the different strains in the

757 phagolysosome. B, C) Fluorescence intensity quantification of Lysotracker and
758 LAMP-3 associated with the phagosome of *M. tuberculosis Mtb*H37Rv (circles),
759 *Mtb*Δ*fasR* (squares) and the complemented *fasR* strain *Mtb*Δ*fasR*-*cfasR*
760 (triangles). Data were expressed in arbitrary units (a.u.). Fiji software was used for
761 quantification. Data represent means ± SEM of three independent experiments.
762 Asterisks indicate significance: *, P ≤ 0.05; **, P ≤ 0.01; and ***, P ≤ 0.001. Data
763 were analyzed using a two-tailed Student *t* test.
764

765 **Fig 8. FasR is essential for the multiplication of mycobacteria in mouse**
766 **lungs.**

767 Three groups of BALB/c mice (10 per group) were infected intratracheally with 10^2
768 CFU of *Mtb*H37Rv, *Mtb*Δ*fasR* and *Mtb*Δ*fasR*-c*fasR* strains and 60 days post-
769 infection bacterial loads in lungs were determined by plating serial dilutions on
770 Middlebrook 7H10 complete agar medium. The graph shows the mean values and
771 error bar of CFU. Data were analyzed using one-way ANOVA analysis and
772 Bonferroni's post-test. (**, P <0.01; ***, P ≤ 0.001).

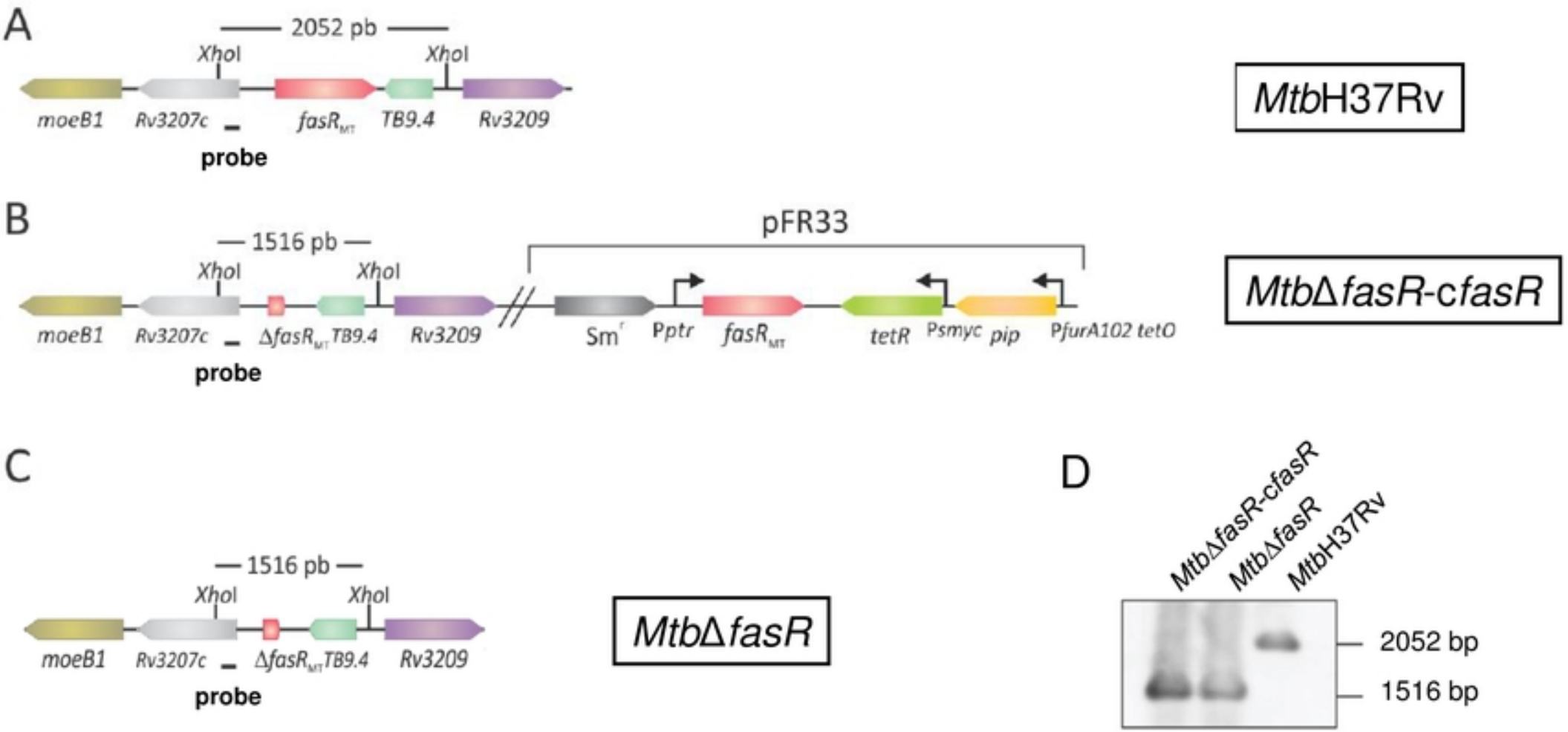

Fig 1. Schematic representation of the genetic organization of the chromosomal region of *fasR*.

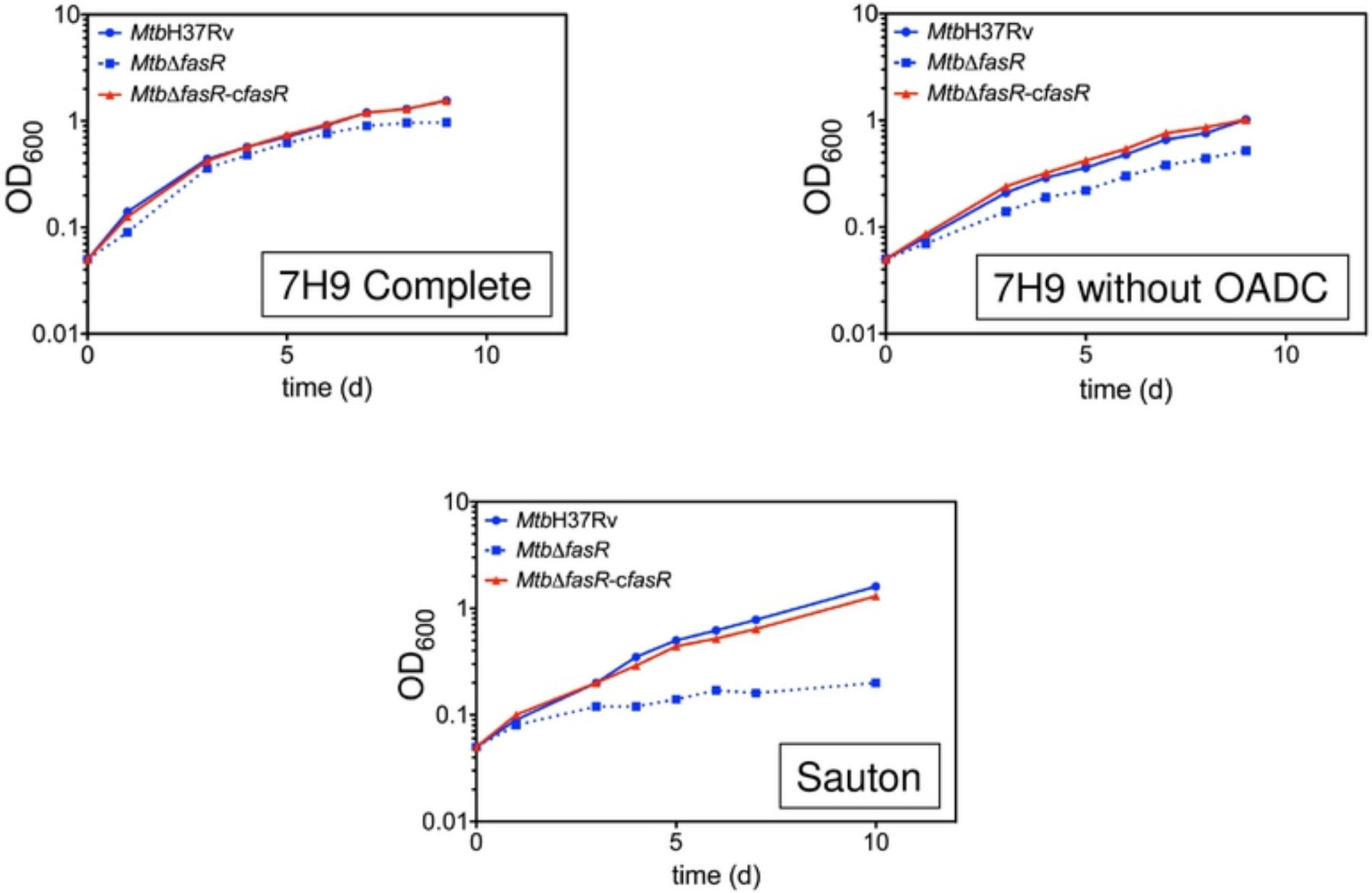

Fig 2. Growth of *M. tuberculosis* strains.

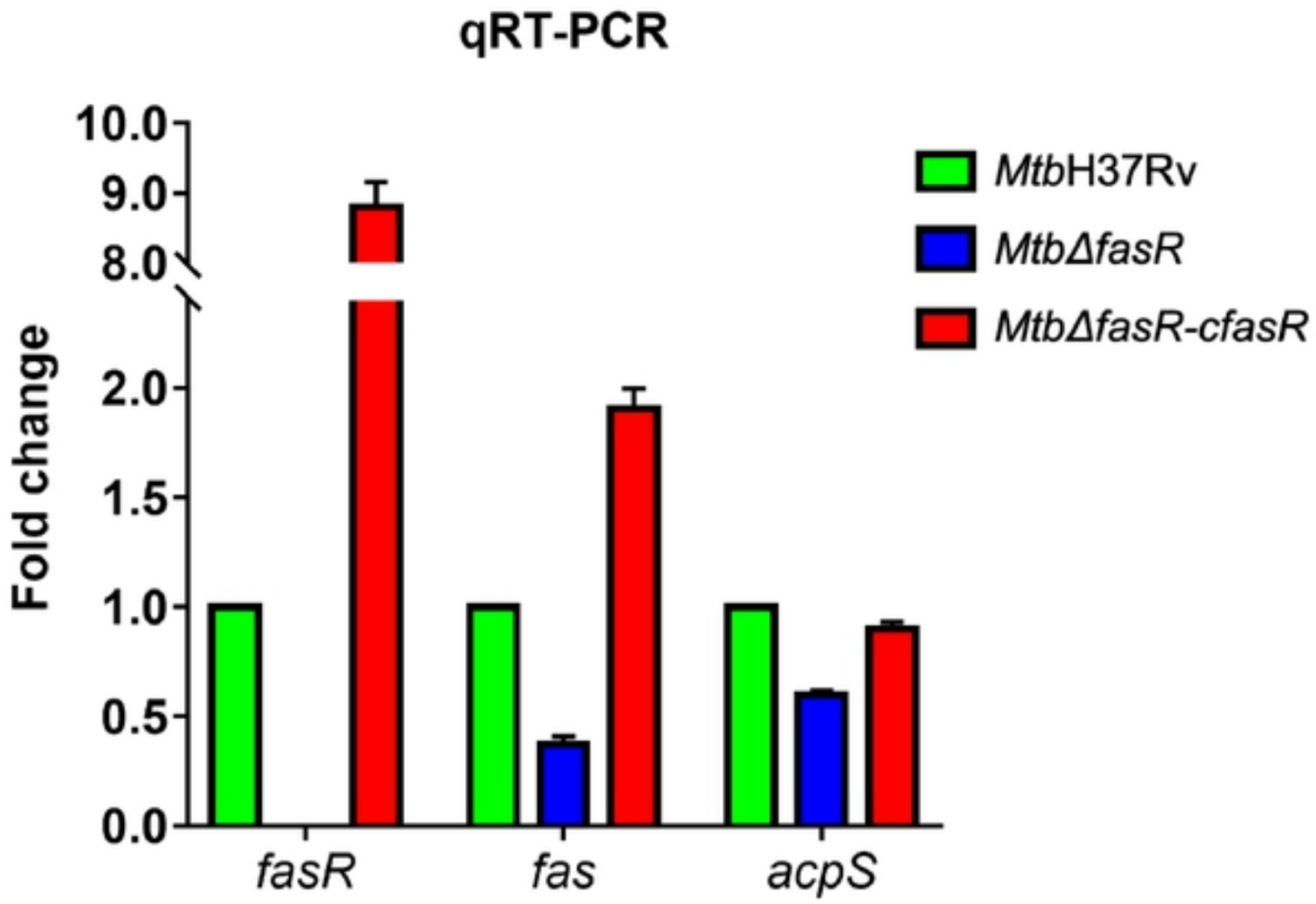

Fig 3. Relative expression levels of *fasR*, *fas* and *acpS* mRNAs measured by quantitative RT-PCR.

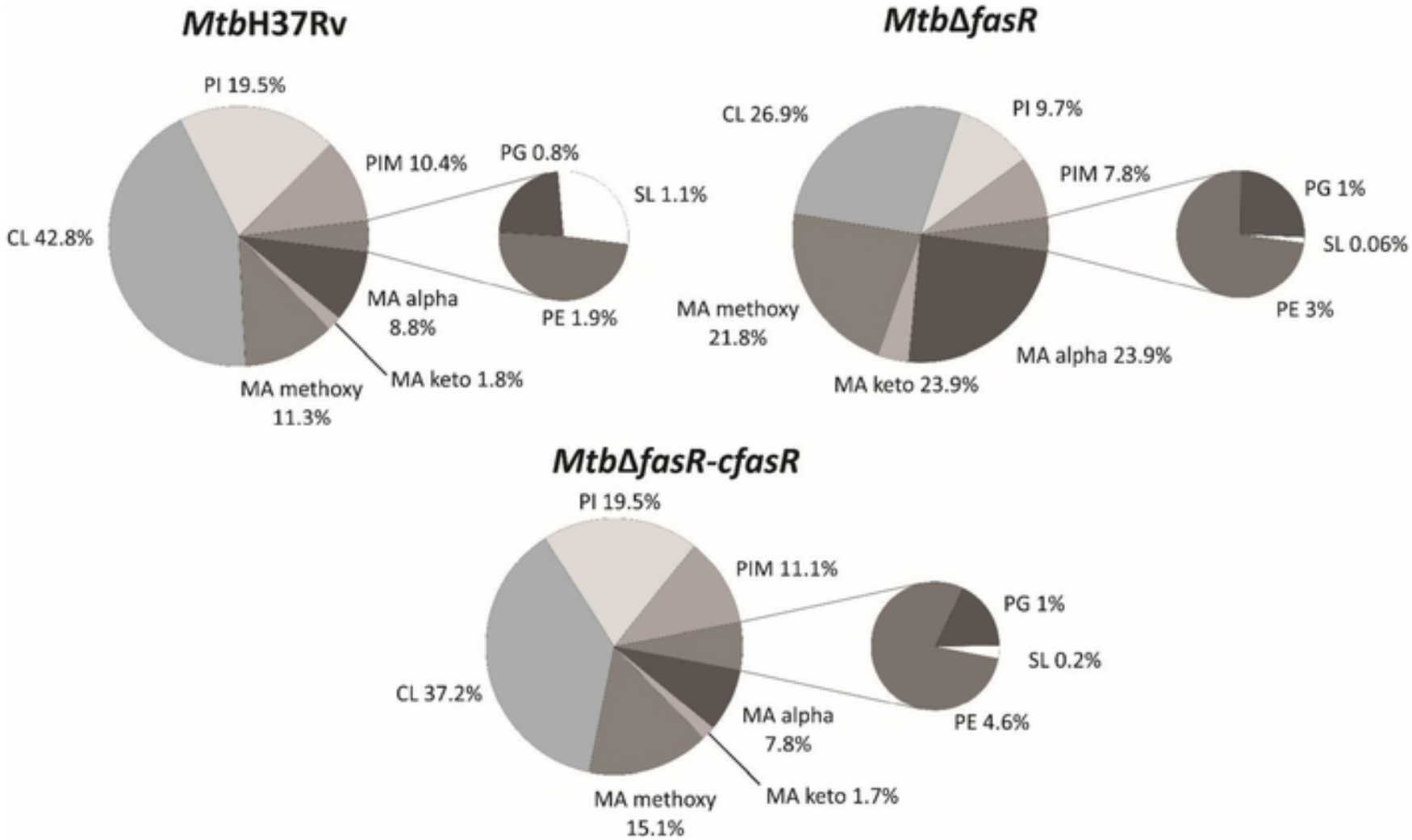

Mycolic acids		Phospholipids	
*Mtb*H37Rv	25%	*Mtb*H37Rv	75%
MtbΔfasR	50%	*MtbΔfasR*	50%
MtbΔfasR-cfasR	22%	*MtbΔfasR-cfasR*	78%

Fig 4. Lipid profile in negative ion mode

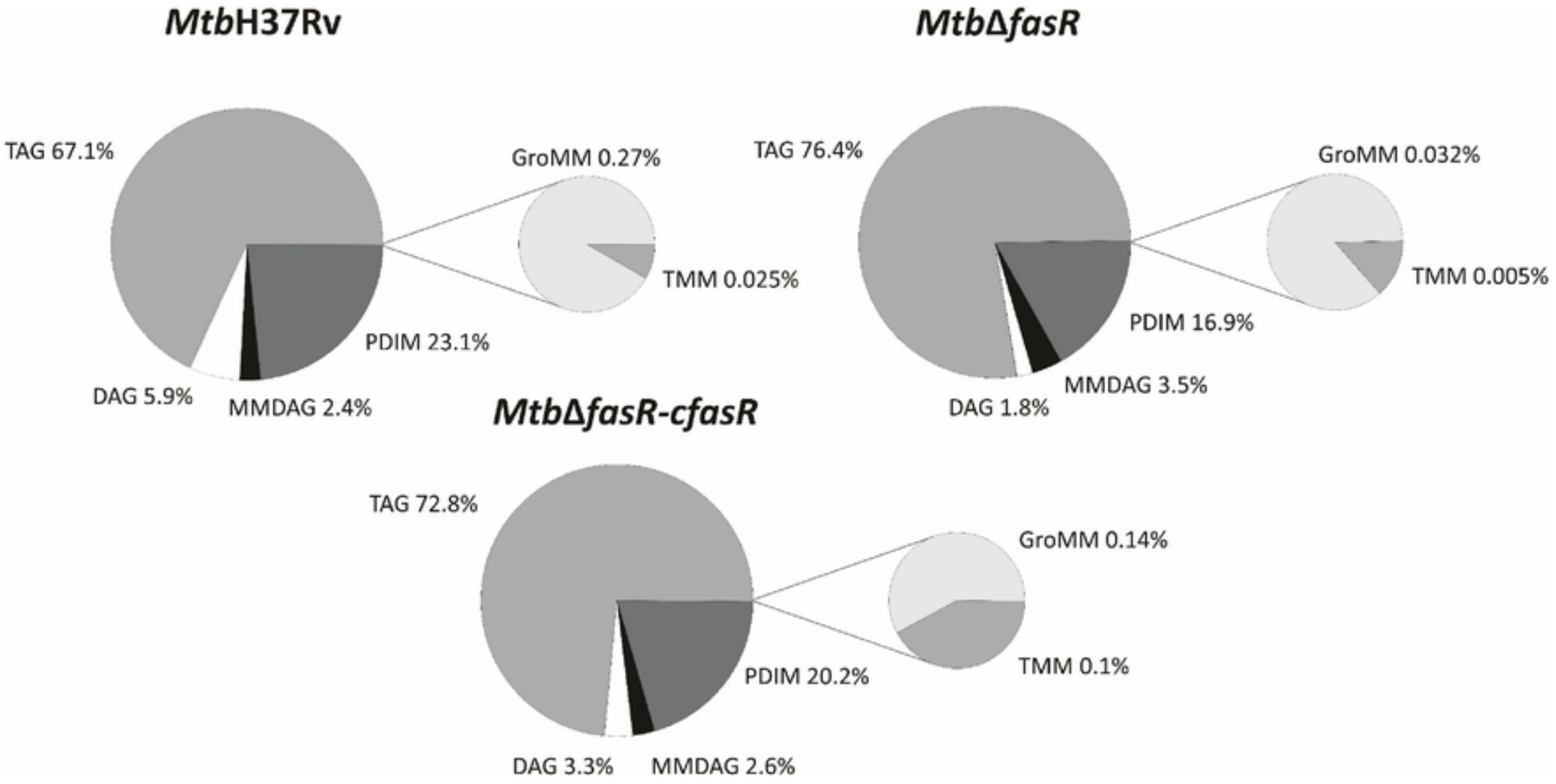

Fig 5. Lipid profile in positive ion mode

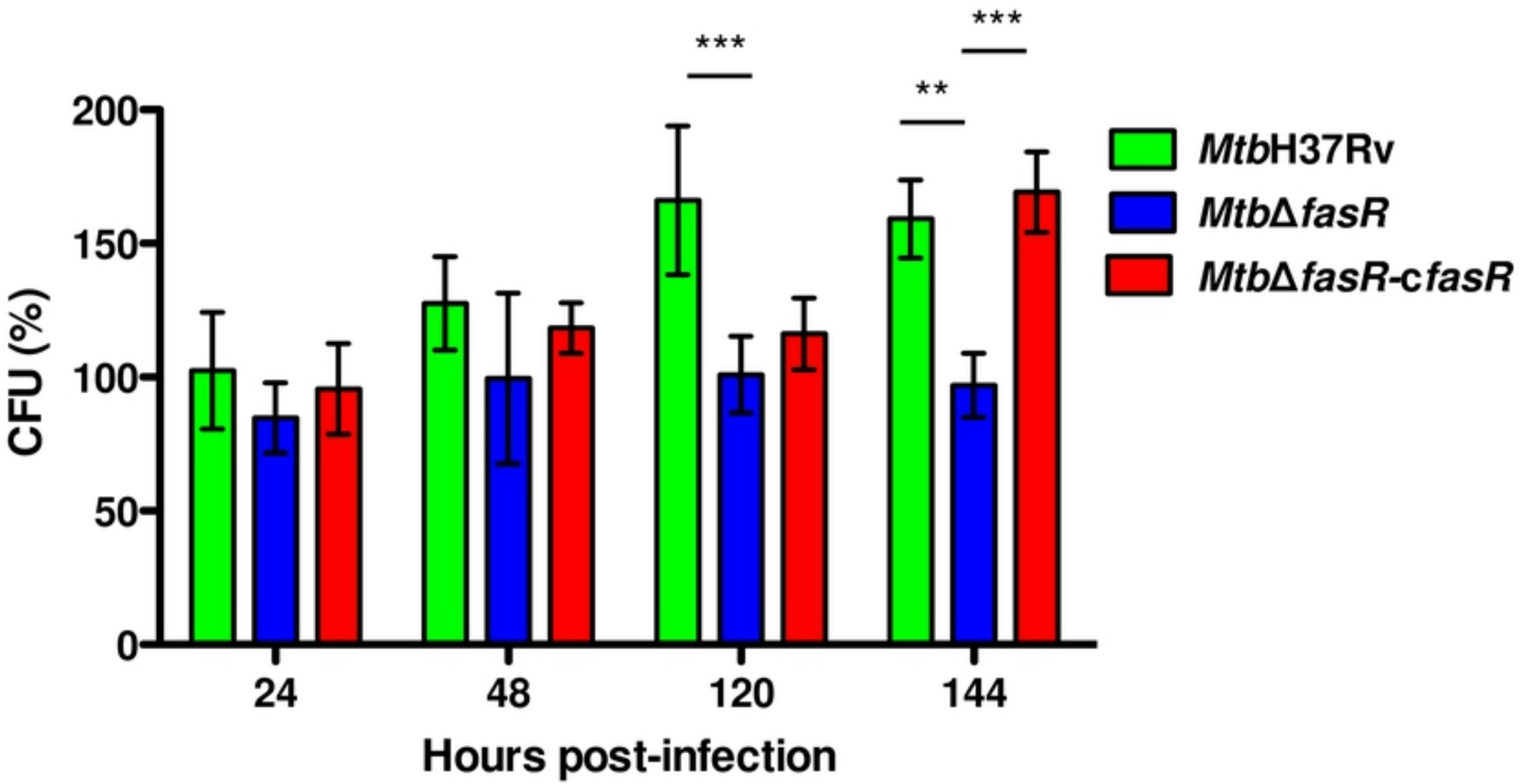

Fig 6. FasR is required for the intracellular survival of *M. tuberculosis*.

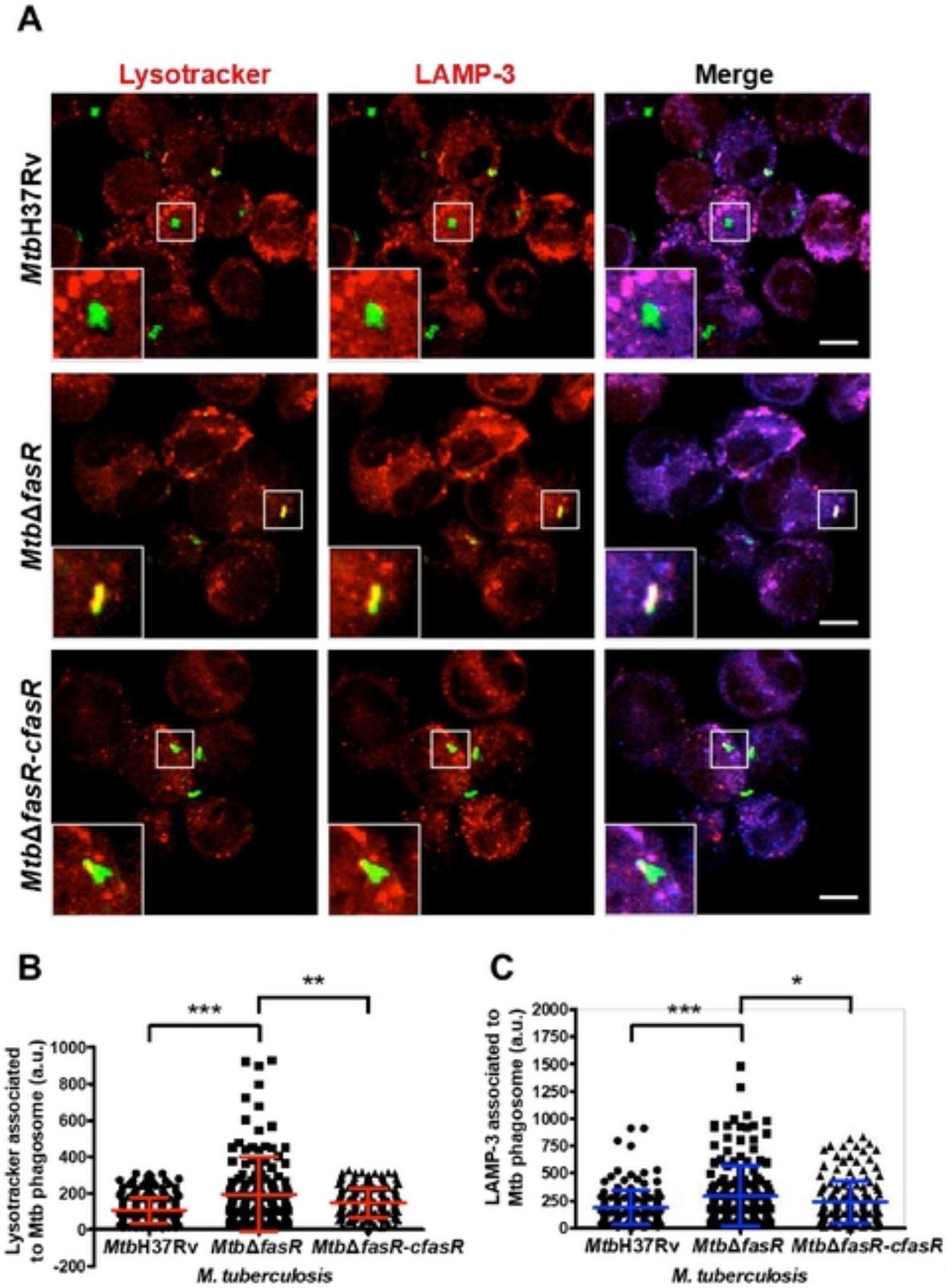

Fig 7. FasR regulates phagosome maturation in macrophages.

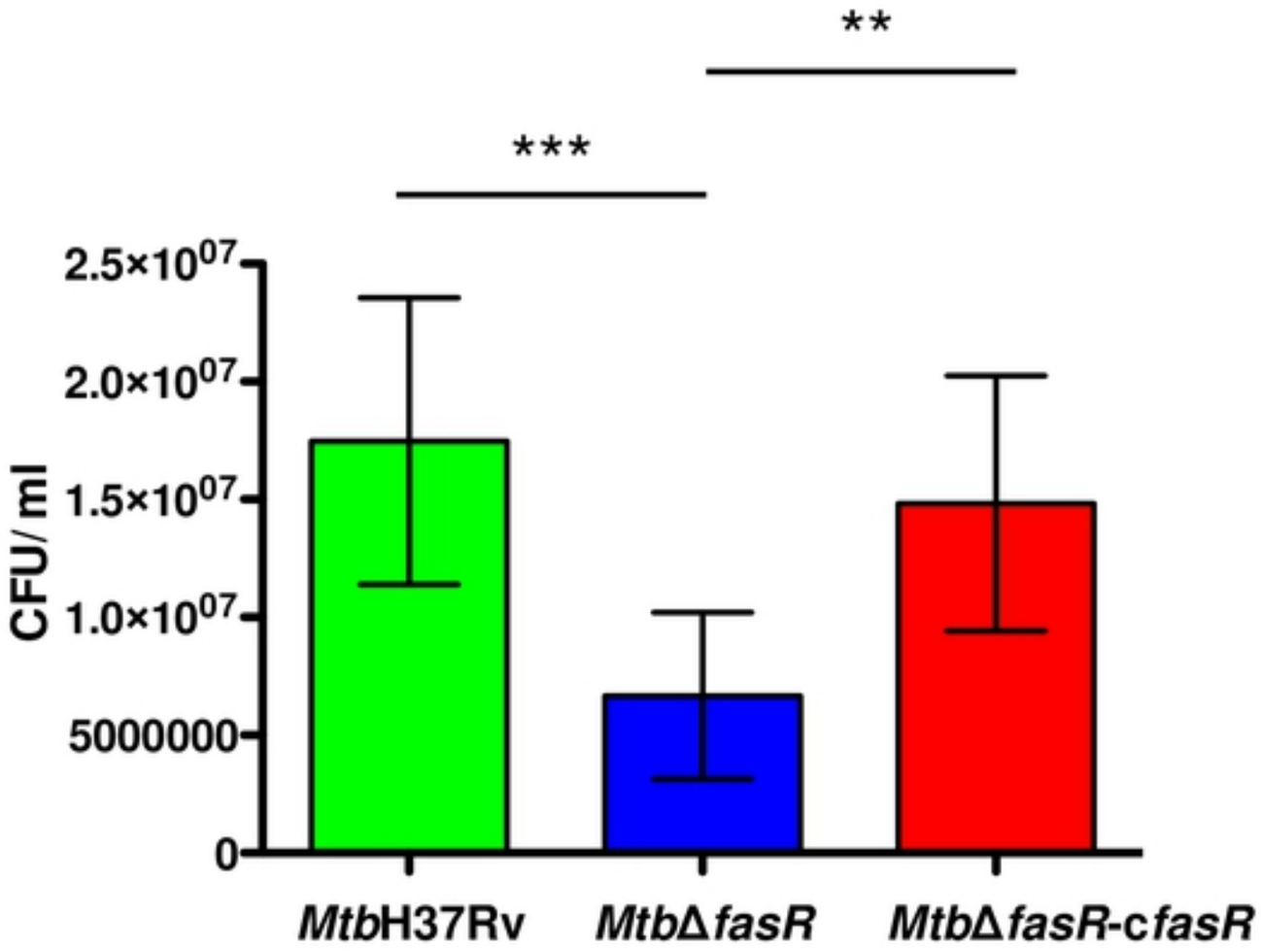

Fig 8. FasR is essential for the multiplication of mycobacteria in mouse lungs.